

Wide-bandwidth electro-mechanical actuators for tunneling displacement transducers

T.W. Kenny*, W.J. Kaiser**, H.K. Rockstad, J.K. Reynolds, J.A. Podosek, and E.C.

Vote

Center for Space Microelectronics Technology

Jet Propulsion Laboratory

California Institute of Technology

Pasadena, CA 91109

Abstract

A series of displacement transducers have been demonstrated which are based on the detection of electrons that quantum-mechanically tunnel across a narrow gap between electrodes. These transducers have important applications due to the sensitivity of the tunneling mechanism to sub-Å variations in the electrode gap. In this paper, we describe the recent development of wide-bandwidth electro-mechanical actuators and simple feedback circuitry which have been adapted for use in tunneling displacement transducers. With these actuators and circuits, we have built tunneling transducers with control bandwidths well in excess of 10 kHz. The design, fabrication, operation and applications of these actuators are described.

The authors may be reached:

T.W. Kenny Phone : (415) 725-3805, Fax : (415) 723-3521,

kenny@sunrise.stanford.edu

W.J. Kaiser Phone : (818) 354-8238, Fax : (818) 393-4540

kaiser@seas.ucla.edu

Displacement transducers are frequently used in sensors for the detection of physical signals. For the purposes of this discussion, we shall consider the displacement transducer to be the element of the sensor which detects the deflection of another sensor element, and produces an electrical signal proportional to that displacement. For example, many accelerometers operate by using a conventional displacement transducer (capacitive, inductive, optical) to detect the deflection of an elastically supported proof mass. The performance (resolution, bandwidth, dynamic range) and operating requirements (size, mass, power consumption) are often dictated by those of the transducer. In addition, well-known scaling laws have been established which relate the performance of these conventional transducers to their characteristics, such as volume, mass, and power consumption. As a result, many sensors based on conventional transducers have already been miniaturized as far as allowed by the scaling laws.

We have investigated the use of electron tunneling across a narrow barrier between metallic electrodes as a displacement transducer. In some cases, the tunneling transducer can be expected to offer substantial advantages over conventional transducers in terms of performance and operating requirements.

Electron tunneling was originally developed for use in microscopy.¹ As shown in the early work on the Scanning Tunneling Microscope (STM), the current due to the tunneling of electrons across a narrow barrier of width s is given by :

$$I \propto V \exp(-\alpha \sqrt{\Phi} s), \quad (1)$$

where Φ is the effective height of the tunneling barrier, V is the bias voltage (small compared to Φ), and $\alpha = 1.025 (\text{\AA}^{-1} \text{ eV}^{-1/2})$. For typical values of Φ and s , (1 eV and 10 \AA , respectively) the current varies by a factor of three for each \AA change in electrode separation. For this situation, an electronic circuit capable of detecting 1% variations in a 1 nA current from a 100 M Ω source would be good enough to detect deflections as small as 0.003 \AA . If the detection were limited by shot noise in the tunnel current, the minimum detectable deflection would be $1.2 \times 10^{-5} \text{\AA}/\sqrt{\text{Hz}}$.

It is especially important to note that the displacement responsivity of the tunneling transducer is not directly dependent on the dimensions of the transducer. As a result, the tunneling transducer may be miniaturized without loss of displacement resolution. This

development creates an opportunity for miniaturization of a broad class of sensors without loss of performance. A position sensor based on electron tunneling has already been incorporated into the design for an accelerometer,²⁻⁴ an infrared sensor,^{5,6} and a magnetometer.⁷ Several other applications are being considered as well. In addition, MacDonald and coworkers have developed single crystal-based fabrication techniques for miniaturized tunneling structures,⁸⁻¹⁰ and Fujita and coworkers have utilized surface micromachining to construct an operational lateral tunneling sensor.¹¹ Theoretical issues surrounding the fundamental limits to displacement detection with tunneling transducers have also been studied.¹²⁻¹⁵ Many of the fundamental issues, engineering issues and applications associated with tunneling sensors were recently discussed at the first Tunnel Sensors Workshop.¹⁶

Because tunneling only occurs when the tip is nearly 10 Å from the counterelectrode, the gap between the electrodes must be controlled by feedback during operation. This is usually accomplished by measuring the tunneling current, comparing it to a reference value, and applying correction signals to an electromechanical actuator. This actuator may function by applying forces to the moving sensor element so as to keep the tip-element gap constant (force-rebalance design), or by applying forces to a transducer element so as to make the tip 'follow' the moving sensor element (dual-element design). If the gain of the transducer/circuit/actuator is sufficient, the tunneling current will be maintained in the presence of external disturbances. By monitoring the feedback signals produced by the control circuit, one can detect the forces applied to the sensor element (force-rebalance design) or detect the deflection of the sensor element (dual element design). One advantage of the dual-element design is the possibility of independent tuning of the actuator and sensor element dynamical characteristics to simplify the design and optimize the performance of the sensor. One disadvantage of the dual-element design is the need to fabricate a second micromechanical element with electrodes.

Through use of the tunneling transducer, the extreme sensitivity to displacement allows the amplification and measurement of small deflections with relatively simple circuitry. As a result, the characteristics of the electromechanical actuator used to control the separation between the tunneling electrodes often impose the dominant limitations to the performance of the tunneling system. For example, piezoelectric actuators are favored for STM applications because they may be easily configured to provide lateral scanning in

addition to precise vertical control. However, piezoelectric actuators suffer from sensitivity to temperature, hysteresis, and creep. STM instrument manufacturers have solved these problems by calibration and compensation techniques, but these techniques are inappropriate for many sensor applications because of complexity and cost.

For the application of tunneling as a displacement transducer, it is important that the characteristics of the actuator are compatible with the measurement requirements. In particular, the actuator must have adequate bandwidth, dynamic range and precision to perform the measurement of interest. In contrast to STM, it is not necessary for the actuator to allow lateral scanning, nor is it necessary to allow a mechanism for replacing tips and samples. Because of these considerations, piezoelectric actuators are not ideal for tunneling sensors. Instead, we have developed actuators which are fabricated entirely from micromachined silicon components, and use electrostatic deflection to control their position. Silicon micromachining offers the capability for micrometer control over the shape of micromechanical structures, and the opportunity to fabricate the majority of the micromechanical structure from silicon.

It is important for any transducer to be insensitive to environmental sources of noise. For example, an infrared detector based on a tunneling displacement transducer should be insensitive to vibration. As is well known, early STMs were extraordinarily sensitive to vibration, and required the construction of large, complex vibration isolation systems for their use. In order to adapt tunneling for use as a transducer for sensor applications, the built-in sensitivity to vibration, as well as other environmental stimuli such as temperature and pressure, must be reduced. Since the tunneling transducer is fundamentally a mechanical structure, the sensitivity to vibration is best eliminated through careful mechanical design. When a mechanical element is subjected to an acceleration at frequencies below its resonance, the amplitude of deflection is inversely proportional to the square of the mechanical resonant frequency. Therefore, sensitivity to vibration is best reduced by increasing the mechanical resonant frequency of all elements of the transducer. It is also important to reduce the sensitivity of the transducer to temperature. By using electrostatic deflection of micromechanical structures, we capitalize on the insensitivity of electrostatics to temperature, and the weak sensitivity of mechanical characteristics, such as Young's Modulus, to temperature.

The original tunneling sensors based on the use of micromachined actuators with electrostatic deflection consisted of low-stiffness structures to allow their deflection over a considerable range ($>100 \mu\text{m}$).³ These large deflections were necessary to achieve the 'coarse approach' as well as the 'fine control' with a single technique. Prototype transducers based on this design were operated and characterized. These prototype devices were based on simple micromachining techniques, and consisted of folded cantilever springs with a total mass of about 30 mg, and a total area of about 2 cm^2 . Displacement sensitivities approaching $0.001 \text{ \AA}/\sqrt{\text{Hz}}$ were measured with these prototype tunneling transducers.

The requirement for deflection over a considerable range with electrostatic forces led to a need for soft mechanical suspension for the moving transducer element and to resonant frequencies of less than 200 Hz. To achieve stability in the control of these elements, the bandwidth of the feedback control system was restricted to less than this resonant frequency. Many external stimuli, such as laboratory accelerations, contained components outside the 200 Hz bandwidth. These higher frequency excitations caused variations in the tip-counter-electrode separation that were not countered by the feedback circuit, and occasionally led to 'crashing' of the tip into the counter-electrode. In these devices, the tip was attached to the 30 mg actuator element, and the counter-electrode was supported by a solid substrate, so damage in the form of removal of the gold or even crushing of the tip was possible, and would result in the failure of the sensor.

Many important signals include components at frequencies above 100 Hz. Examples include audio pressure signals, mechanical vibrations, and infrared signals from spectrometers. To enable sensing of signals above 100 Hz with tunneling transducers, we have begun using a new series of micromachined actuators. These new actuators are important because they are designed to offer resonant frequencies above 10 kHz. The new actuators achieve the higher resonant frequencies primarily through substantial reduction in actuator mass. As a result, the new actuators have smaller range of deflection ($<5 \mu\text{m}$), which precludes their use for coarse approach between tunneling electrodes. Using silicon micromachining techniques to better define the initial separation between the tunneling electrodes, it is possible to accomplish the needed coarse approach during assembly.

Two different types of wide-bandwidth actuator have been designed and tested. The first of these consists of a small micromachined cantilever. Several techniques are

available for the fabrication of suitable cantilevers.¹⁷ In order to precisely control the cantilever thickness, an etch-stop is required. For our studies, we have obtained commercially prepared silicon wafers with a 4 μm thick layer of heavily doped silicon grown epitaxially on one surface. The chemical etch rates for heavily doped silicon in common etchants such as Ethylenediamine Pyrocatechol (EDP) are as much as 3 orders of magnitude smaller than for intrinsic silicon. Lateral patterning of the cantilever is achieved by plasma etching techniques that are less selective. This actuator was designed for an accelerometer application with a specified measurement bandwidth of 5 kHz.

The cantilever's dimensions are 0.7mm x 0.7 mm x 4 μm . Given these dimensions, its resonant frequency and stiffness may be calculated and are 37 kHz and 17 N/m respectively.^{18,19} This actuator is used as the control element of a miniature, dual-element accelerometer, whose design concept is shown in Fig. 1. This accelerometer operates by using the wide-bandwidth cantilever to follow the motion of the suspended proof mass at all frequencies below the resonant frequency of the cantilever. The use of a separate transducer element to follow the motion of the proof mass is driven by the need for measurements of acceleration both below and above the resonance of the proof mass. The design, fabrication and characterization of this accelerometer will be described elsewhere.²⁰

The second wide-bandwidth actuator consists of a diaphragm. These diaphragms are fabricated by coating the front surface of a silicon wafer with low-stress LPCVD silicon nitride. The diaphragms are released by etching square holes through the wafer from its back surface with a chemical etchant that does not etch silicon nitride, such as EDP, and then coated with 2000 \AA of Au. A drawing of a diaphragm positioned above the tunneling and deflection electrodes is shown in Fig. 2. This actuator was designed for an infrared detector that will be used to detect variations in infrared power at modulation frequencies of up to 10 kHz. For the infrared sensor, the dimensions of the membrane are 2mm x 2 mm x 0.7 μm . A series of concentric circular corrugations with an inside radius of 0.5 mm are used to release the remaining tensile stress. It is expected that the dynamical characteristics of the diaphragm will be dominated by the unstressed region. The resonant frequency and stiffness for an unstressed circular diaphragm of these dimensions are calculated to be about 18 kHz and 4 N/m respectively.²¹ The linear range of deflection for this actuator may be extended by corrugation of the diaphragm. The fabrication and characterization of the infrared sensor will be described elsewhere.²²

One important advantage to the use of the cantilever or the membrane as a tunneling contact is that these elements are not rigid and do not carry much momentum. Therefore, the amount of force between the tunneling electrodes during a 'crash' is limited. During the operation of sensors with the wide-bandwidth actuators, there have been no sensor failures related to wear or damage at the electrodes. For use of tunneling as a transducer in any practical application, we strongly recommend that one of the contacts be supported by a compliant element.

In both of these devices, a micromachined silicon tip is fabricated on a silicon wafer by undercutting a $25\mu\text{m}$ square of mask material with an anisotropic etchant. This same process step forms the recess which contains the tip and deflection electrodes. After etching, these surfaces are passivated with $1\mu\text{m}$ of thermally-grown SiO_2 , and a gold electrode pattern is created by a modified liftoff technique. An SEM micrograph of a typical tip and electrode pattern that results from this process is shown in Fig. 3. It is important to note that we do not employ any tip sharpening techniques. We have found that, for the purposes of a z-component transducer, controlling the "sharpness" of the tip is not important for controlling sensor performance. We have used tips such as the one shown in Fig. 3, which has a radius of curvature of $1\text{-}5\mu\text{m}$, or we have used tips which have a $5\mu\text{m}$ flat mesa on the end. Sensors with 'sharp' or 'flat' tips have had indistinguishable behavior and performance. The exponential nature of the tunneling process virtually guarantees that the observed current will be dominated by individual atoms on the tunneling electrodes, whatever the shape of the electrode surfaces.

Since tunneling takes place between the atoms on the surfaces of the tunneling electrodes, it is critically important that the electrode material be metallic. In all of our successful experiments, we have utilized Au films as tunneling electrodes. Au is a nearly ideal metal for this purpose because it does not undergo chemical reactions to form insulating surface layers when exposed to air. Most other metals utilized for STM tips (W, Pt-Ir, ...) have reactive surfaces which may require specialized cleaning treatments under Ultra-High Vacuum (UHV) conditions to allow stable tunneling. For the purposes of sensor applications, it will be impractical to maintain UHV conditions at the tunneling electrodes during manufacturing, assembly, and operation. Therefore, we have concentrated on development of Au-based electrode processing techniques which allow long-term, trouble-free operation of the tunneling electrodes in air at atmospheric pressure.

The original tunneling sensors were metallized by e-beam evaporation of pure Au films through micromachined shadow masks onto the oxide-passivated silicon surfaces. More recently, a liftoff-based lithographic technique has been developed which allows much higher density electrode patterns. In liftoff, photoresist is patterned, metal is deposited, and the photoresist is dissolved, 'lifting' the parts of the pattern that were deposited on photoresist. Since liftoff requires strong adhesion between the Au and the SiO₂ coating on the tip and surrounding surfaces, it is common to utilize an intermediate adhesion layer. For example, a 100Å Cr layer may be deposited on the surface before the gold deposition. The first Cr atoms arrive at the surface and react to form Cr₂O₃, which is strongly bound to the SiO₂ surface. The last Cr atoms remain as metallic Cr, and can form strong bonds to the first Au atoms. Unfortunately, we have found that some of the Cr can diffuse to the surface of the Au film, where it forms an oxide which prevents the sensor from tunneling. Devices fabricated with Cr adhesion layers were found to operate poorly after fabrication, and stopped working altogether within a week of the evaporations. X-ray Photoemission Spectroscopy (XPS) indicated the presence of Cr₂O₃ on the surface of these devices. We have found that deposition of a Ti adhesion layer followed by a Pt diffusion barrier layer, and the Au layer results in clean tunneling electrodes. In this case, the Pt layer is thermodynamically stable, and prevents the migration of Ti through to the gold surface. Tunneling sensors based on this electrode combination have already been operated for as long as 18 months in air without evidence of electrode degradation. Other combinations of adhesion layers and diffusion barriers can be made to work, but it is important to guard against the possibility of contaminant diffusion to the Au surface.

Conventional STM feedback loops must control complex electromechanical structures with low frequency resonances. The design and operation of these feedback loops are complicated by the presence of low-frequency resonances because of the related distortions in the response spectrum. In these new wide-bandwidth actuators, the lowest mechanical resonant frequency is above 10 kHz. Therefore, the gain and bandwidth of the electrical circuit used to control the sensor may be substantially larger than that used in typical STMs or in previous tunneling sensors. Because of this, the feedback circuitry used may be simplified. Figure 4 shows a typical feedback circuit that has been used to control tunneling between a micromachined tip and the diaphragm actuator.

Both of these devices are operated in the following manner: A 150 mV tunneling bias is applied to the electrode on the actuator, and the electrode on the tip is grounded through a 10 M Ω resistor. A large voltage is applied to the deflection electrodes, electrostatically attracting the membrane down towards the tip. When the membrane is within 10 Å of the tip, a tunnel current of 1.5 nA appears. A voltage drop across a 10 M Ω resistor in series with the tip arises whenever tunneling occurs. A low-noise operational amplifier in follower configuration is positioned near the transducer to lower the source impedance for measurement of the tunneling current. A single op-amp is then used to compare the preamplifier output with a set-point and generate an error signal. This low-voltage, wide-bandwidth error signal is then added to a high-voltage, narrow-bandwidth offset to produce the voltage that is applied to the deflection electrodes. The high voltage signal may be generated by a power supply that is initially adjusted to set the error signal near zero.

In this configuration, the output of the first preamplifier never exceeds the range between the bias voltage of 163 mV and ground. We have found this preamplifier configuration to be more stable than other possible circuits, such as a virtual ground configuration that drives the preamplifier output to the supply voltage rail in the presence of a sensor overdrive. If the error amplifier is positioned near the transducer, the preamplifier may be eliminated. The resulting feedback circuit requires only a single operational amplifier, an external offset voltage, and a few fixed-value resistors.

A CA3140 amplifier is used for both the preamplifier and the error amplifier in the circuits studied in this work. Other FET-input amplifiers may be used as well. The input impedance of the first amplifier should be substantially higher than the 100 M Ω source impedance of the transducer. Also, the input current noise of the amplifier should be low enough that it does not dominate the final noise of the sensor. The CA3140 has input noise of 2×10^{-13} A/ $\sqrt{\text{Hz}}$, which is lower than other noise sources that we have observed in operation of these sensors. Since the noise and bandwidth in these systems have not been limited by preamplifier characteristics, we have not been generally concerned with optimization of these elements.

These transducers were made operational and routine characterizations were carried out. For all the measurements described in this report, the transducer was operated in laboratory air at atmospheric pressure. Stable tunneling was achieved in a typical

transducer with an average deflection voltage of 120 V. Figure 5 shows a measurement of the voltage noise from the feedback circuit measured at the output of the error amplifier, and at the transducer deflection electrode for a membrane transducer. The signal at the deflection electrode is smaller at higher frequencies because of the low-pass filter which consists of the resistor network in the feedback loop and the stray capacitance at the deflection electrode.

This noise spectrum exhibits a typical $1/f$ character, in agreement with tunneling noise spectra seen elsewhere.²³⁻²⁵ The source of the $1/f$ noise in these devices has not been experimentally determined. Migration of individual gold atoms at room temperature has been observed in STM experiments. Others have attributed noise in tunneling in air to migration of adsorbed water molecules through the tunneling region. Either of these mechanisms can be expected to produce randomly-timed steps in the feedback signal, which could be expected to produce the shape of the observed spectrum. Also, relaxation of the package which holds the two elements of the structure can also be expected to introduce low frequency noise. Finally, we have observed that building pressure fluctuations from the air handlers in the adjacent clean room can be a source of low frequency noise in our measurements. Packaging the sensors in air-filled, stiff-walled containers often results in reduction in the observed noise spectrum. Studies of noise in these devices are continuing at JPL and elsewhere.

It is necessary to perform an independent measurement of transducer stiffness to convert noise in the feedback signal to errors in the position measurement. We have used a laser interferometer²⁶ to measure electrostatically-induced deflections of the membrane near the operating voltage. A typical sensor was brought into tunneling at an average deflection voltage of 120 V. The deflection voltage was reduced to 110 V, and a 5 V, 40 Hz sinusoidal oscillation was added to the 110 V offset. The resulting oscillation in the deflection of the membrane was measured with the laser interferometer, which recorded an amplitude of 400 Å. Therefore, the transducer responsivity is given by :

$$\frac{\partial s}{\partial V} = \frac{400 \text{ Å}}{5 \text{ V}} = 80 \text{ Å/V} \quad (2)$$

With the measured voltage noise of the transducer operating in air in the laboratory as shown in Fig. 4, the displacement resolution may be calculated. The measured

displacement resolution of this transducer is then $0.007 \text{ \AA}/\sqrt{\text{Hz}}$ at 10 Hz and less than $0.0001 \text{ \AA}/\sqrt{\text{Hz}}$ at 10 kHz. The interferometer measurement is independent of oscillation frequency to beyond 2000 Hz, indicating that squeeze film damping does not affect the dynamics of the diaphragm at these frequencies.

The measured deflection of $80 \text{ \AA}/\text{V}$ corresponds to a membrane stiffness of about 30 N/m , which is substantially larger than the calculated value of 4 N/m .²¹ The discrepancy is likely due to remaining tensile stress in the diaphragm, the added stiffness of the Au film, and contributions from non-bulk effects.

Measurements of the effective tunnel barrier height, ϕ , are an important indication of the cleanliness of the tunneling electrodes. For tunneling between clean gold electrodes in air, values for ϕ of between 0.05 and 0.5 eV are to be expected. The tunneling barrier height was measured in the following manner: A 1 mV, 10 Hz oscillation voltage was added to the reference input of the feedback loop, causing the feedback loop to modify deflection voltages so as to produce a 0.1 nA oscillation in the tunneling current. To produce this oscillation, the feedback loop adds a small voltage oscillation to the deflection voltage, which was measured to be 2 mV in amplitude at the output of the op-amp. From Eq. 1, the height of the tunnel barrier, ϕ , is given by :

$$\sqrt{\phi} = \frac{-1}{\alpha I} \frac{\partial I}{\partial s} = \frac{-1}{\alpha I} \frac{\partial I}{\partial V} \frac{\partial V}{\partial s} = \frac{1}{1.025 \times 1.5 \text{ nA}} \frac{0.1 \text{ nA}}{0.002 \text{ V}} \frac{1}{80 \text{ \AA}/\text{V}} \quad (3)$$

$$\phi = 0.17 \text{ eV.}$$

At different times and with different sensors, this measured barrier height may vary by as much as a factor of 5.

The effect of variations in barrier height is explained as follows: It is important to remember that the feedback loop applies rebalance forces to maintain the position of the membrane. In this case, the system will provide feedback signals as needed to keep the position of the membrane very nearly constant in the presence of external forces. Since the feedback force necessary to achieve balance is always very nearly equal to the signal force, regardless of the actual value of the barrier height, the responsivity should stay approximately constant. For example, if the gain in the system is 100 at the signal

frequency, a 2x reduction in the barrier height will produce a change in responsivity, R, given by :

$$R = R_0 \left(1 - \frac{\sqrt{2}}{100} \right) = (0.986) R_0, \quad (4)$$

or less than a 2% reduction. This is a general property of force-rebalanced sensors, and explains why force rebalance designs are in wide use for precision measurements of physical signals. The signal/noise ratio for the tunnel transducer system is affected by variations in the barrier height, because the noise is proportional to the reciprocal of the square root of the barrier height. For this reason, it is important to use electrodes which offer reasonably high barrier height under operating conditions. For tunneling in air, Au films are the best available choice.

Figure 6 shows a measurement of the bandwidth of the transducer. For this measurement, a white noise voltage modulation is added to the reference input of the error amplifier in the feedback loop. The feedback loop responds by generating an amplified modulation signal at the deflection electrode, which produces modulations in the position of the membrane, as well as modulations in the tunneling current. Within the bandwidth of the transducer system, the measured modulation will match the amplitude and phase of the reference modulation. Figure 6 shows the ratio of the measured modulations to the reference modulation as a function of frequency, recorded by a standard spectrum analyzer. At all frequencies up to 50 kHz, the transducer is able to accurately reproduce the reference modulations. Above 50 kHz, this response begins to roll off because of the limited bandwidth of the preamplifier. Figure 7 shows the phase shift between the measured modulations and the white noise modulations. This phase shift is less than 5 degrees for frequencies below 10 kHz, increasing to 30 degrees at 50 kHz. At frequencies above 100 kHz, capacitive coupling between the noise source and the transducer contributes to the measurement, as evidenced by the variation in the phase shift at those frequencies. There was no evidence for the mechanical resonance of the membrane in these measurements.

Some informal life-testing experiments have been carried out on these transducers. For membrane transducers fabricated as described above, an individual device has been in continuous operation for more than 18 months with no observable degradation in performance. An infrared sensor based on this device has been in continuous, unprotected

operation in the lobby of the JPL MicroDevices Laboratory for more than 14 months, where it has been subjected to mostly uncontrolled experimentation (IR signals, shocks, handling, power-supply failures, earthquakes,...). All failures to date for devices of this type have resulted from operator error (mechanical rupture of membrane, application of voltage to the wrong leads). We have delivered devices to collaborators at NASA Goddard, Rose-Hillman Institute of Technology, NAWC Warminster, UCLA, Stanford, and some industrial collaborators, all of whom report successful operation. This collection of experience supports the conclusion that reliable, easily operated tunneling transducers can be built and packaged for real applications

In summary, we have constructed a series of tunneling displacement transducers. These transducers are fabricated using silicon micromachining techniques which have been adapted to produce the required electrode cleanliness. The most recent devices, which are based on high-resonant frequency mechanical elements can be used for measurements of displacement signals at frequencies as high as 50 kHz. Sensors based on the use of tunneling transducers with wide control bandwidths are presently being designed, built and tested.

The authors would like to acknowledge a number of helpful conversations with T. VanZandt, L. Miller, S. Manion, L. Bell, A. Milliken, P. Smith, S. Martin, R. Vasquez, F. Grunthaner, M. Roukes, A. Cleland, D. Marcus, T. Gabrielson, R. Muller, P. Maker and M. Hecht.

The work described in this paper was performed by the Center for Space Microelectronics Technology, Jet Propulsion Laboratory, California Institute of Technology and was jointly sponsored by the Ballistic Missile Defense Organization/ Innovative Science and Technology Office, the Defense Advanced Research Projects Agency, the Naval Air Warfare Center, the Army Space Technology Research Office, and the National Aeronautics and Space Administration, Office of Aeronautics, Exploration, and Technology.

References

*Present Address : Department of Mechanical Engineering Design Division, Stanford University.

** Present Address : Department of Electrical Engineering, University of California Los Angeles.

-
- ¹ G. Binnig and H. Rohrer, Scanning Tunneling Microscopy, IBM J. Res. Develop. 30, 355 (1986).
 - ² S.B. Waltman, W.J. Kaiser, An Electron Tunneling Sensor, Sensors and Actuators 19, 201 (1989).
 - ³ T.W. Kenny, S.B. Waltman, J.K. Reynolds, and W.J. Kaiser, Micromachined Silicon Tunnel Sensor for Motion Detection, Appl. Phys. Lett. 58, 100 (1991).
 - ⁴ A.A. Baski, T.R. Albrecht and C.F. Quate, Tunneling Accelerometer, J. of Microscopy 152, 73 (1988).
 - ⁵ T.W. Kenny, W.J. Kaiser, S.B. Waltman and J.K. Reynolds, A Novel Infrared Detector Based on a Tunneling Displacement Transducer, Appl. Phys.Lett. 59 (1991).
 - ⁶ T.W. Kenny, W.J. Kaiser, J.A. Podosek, H.K. Rockstad, and J.K. Reynolds, Micromachined Electron Tunneling Infrared Sensors, Proceedings 1992 IEEE Solid State Sensor and Actuator Workshop, 174 (1992).
 - ⁷ J.H. Wandass, J.S. Murday, and R.J. Colton, Tunneling Magnetometer, Sensors and Actuators 19, 211 (1989).
 - ⁸ N.C. MacDonald, Single-Crystal Silicon Nanomechanisms for Scanned-Probe Device Arrays, Proceedings 1992 IEEE Solid State Sensor and Actuator Workshop, 1 (1992).
 - ⁹ J.J. Yao, S.C. Arney, S.C. and N.C. MacDonald, Fabrication of high-frequency two-dimensional nanoactuators for scanned probe devices, J. MicroElectroMechanical Systems, 1, 14 (1992).
 - ¹⁰ Z.L. Zhang, N.C. MacDonald, Fabrication of sub-micron high-aspect-ratio GaAs actuators, J. MicroElectroMechanical Systems, 2, 66 (1993).
 - ¹¹ D. Kobayashi, T. Hirano, T. Furuhashi, and H. Fujita, An Integrated Lateral Tunneling Unit, Proceedings 1992 IEEE Micro Electro Mechanical Systems Workshop, 214 (1992).
 - ¹² C.Presilla, R. Onofrio, M.F. Bocko, Uncertainty principle noise in vacuum tunneling transducers, Phys. Rev. B 45, 3735 (1992).
 - ¹³ M.F. Bocko, K.A. Stephenson, and R.H. Koch, Vacuum tunneling probe : a non-reciprocal reduced-back-action transducer, Phys. Rev. Lett. 61, 726 (1988).

-
- 14 T.B. Gabrielson, Mechanical-thermal noise in micromachined acoustic and vibration sensors, *IEEE Electron Devices*, 40, 903 (1993).
- 15 B. Yurke and G. Kochanski, Momentum noise in vacuum tunneling transducers, *Phys. Rev. B* 41, 8184 (1990).
- 16 Proceedings of the 1992 Tunnel Sensors Workshop, Jet Propulsion Laboratory, Pasadena, CA, to be published (1992).
- 17 K.E. Petersen, Silicon as a Mechanical Material. *Proc. IEEE* 70, 420 (1982).
- 18 W.C. Young, *Roark's Formulas for Stress and Strain*, 6th ed. (McGraw-Hill, New York 1989).
- 19 The resonant frequency is given by $f = \frac{3.52}{2\pi} \sqrt{\frac{EIg}{wl^4}}$ (from 12, table 36 on p 714), with $E = 1.9 \times 10^{11} \text{ N/m}^2$, $w = 6.4 \times 10^{-6} \text{ kg/m}$, and $I = 3.7 \times 10^{-21} \text{ m}^4$. The stiffness is given by $k = \frac{8EI}{l^3}$ (derived from 12, table 3 on p 102).
- 20 H.K. Rockstad, J.K. Reynolds, T.W. Kenny and W.J. Kaiser, A High-Resolution Miniature Accelerometer Based on Electron Tunneling, to be published.
- 21 The resonant frequency is approximately given by $f = \frac{10.2}{2\pi} \sqrt{\frac{Et^3g}{12wd^4}}$ (from 12, table 36 on p 716) where w is an average of the densities for silicon nitride and gold. The stiffness is given by $k = \frac{64\pi}{12} \frac{Et^3}{r^2}$ (derived from 12, table 24 on p 429)
- 22 T.W. Kenny, W.J. Kaiser, J.A. Podosek, H.K. Rockstad, J.K. Reynolds, E.C. Vote, and L.M. Miller, Uncooled Infrared Sensors Based on Tunneling Transducers, to be published.
- 23 R. Moller, A. Esslinger, and B. Koslowski, Noise in vacuum tunneling, application for a novel scanning tunneling microscope, *Appl. Phys. Lett.* 55, 2360 (1989).
- 24 T. Tiedje, J. Varon, H. Deckman, and J. Stokes, Tip contamination effects in ambient-pressure scanning tunneling microscopy imaging of graphite, *J. Vac. Sci. Technol. A* 6, 372 (1988).
- 25 Ch. Kleint, Surface Diffusion Model of Adsorption-induced field emission flicker noise, *Surf. Sci.* 25, 394 (1971).
- 26 Polytec Laser Vibrometer OVF-501-0, Polytec P. I. Inc., 3152 Redhill Suite 110, Costa Mesa, CA 92626.

Biographies

Thomas W. Kenny is presently an Assistant Professor in Mechanical Engineering at Stanford University, where his research is focused on development of high performance microsensors and on the study of fundamental phenomena in microstructures. He received his B.S. degree in Physics from the University of Minnesota in 1983. His Ph.D research was carried out at UC Berkeley in the Physics Department and was focused on the measurement of the heat capacity of sub-monolayer coverages of noble gas atoms at cryogenic temperatures. Other work at Berkeley was associated with development and use of infrared spectrometers and detectors. After receiving his degree in 1989, Tom joined Bill Kaiser's research group at JPL and began working on the development of tunneling sensors, eventually becoming Group Leader for these activities. This activity has been highlighted by the recent demonstration of high-performance, yet robust and easily operated infrared sensors based on tunneling, for which a 1993 R+D 100 Award was received. Other tunneling sensors being developed include accelerometers and magnetometers. This work at JPL is ongoing, and is shifting focus to design and testing of small-format linear arrays of infrared sensors. Tom is also involved in the development of other sensing and micromachining technologies at JPL, including work in capacitive accelerometers and pressure sensors, deformable optical components, and others. Tom is the author of 5 patent applications and over 25 technical publications and invited presentations.

William J. Kaiser is a Senior Research Scientist and Technical Group Leader at JPL. He received his Ph.D. in Condensed Matter Physics from Wayne State University in Detroit, Michigan in 1984. His graduate work was completed while he was employed at the Physics Department of Ford Motor Co. Research Staff, in Dearborn, Michigan from 1977-1986. While at Ford, Dr. Kaiser's research included several areas in condensed matter physics, and also, the development of a series of automotive sensors. At JPL, he and his group focus on basic research in semiconductor materials and devices and the development of new microinstruments for measurement applications. An emphasis of this group is the development and demonstration of new measurement principles. These include new scanning tunneling microscopy experimental methods for materials investigation. A method developed at JPL by Dr. Kaiser and his group, Ballistic-Electron-Emission-Microscopy (BEEM), has been adapted at laboratories in the U.S., U.K.,

Europe, and Japan. BEEM has been transferred to industry (a commercial BEEM apparatus is available) and has been the subject of four consecutive international meetings. An exciting area of current research is the development of measurement methods which provide compact sensors and instruments with the high sensitivity normally obtained only in large devices. Dr. Kaiser is a member of the American Physical Society and American Geophysical Union. He has six patents and over 80 publications and invited presentations. He and his group have received awards including 1990 and 1993 R&D 100 Awards, a NASA Medal for Exceptional Scientific Achievement (1990), and the Peter Mark Award of the American Vacuum Society (1991).

Howard K. Rockstad is presently working in the tunnel sensor group at the Jet Propulsion Laboratory, with emphasis on the ongoing development of electron tunnel sensors applied to high-sensitivity miniature accelerometers, and has also been part of a novel micromachined silicon neuron probe program. He received his B.A. degree in Physics and Mathematics from St. Olaf College, and his M.S. and Ph.D. degrees in physics from the University of Illinois. His thesis research dealt with optical conversion of color centers in alkali halide crystals at cryogenic temperatures. Subsequent research at Corning Glass Works dealt with high electric field effects in semiconductors, and with electronic properties of amorphous semiconductors. He continued work with amorphous semiconductors at Energy Conversion Devices, Inc. Subsequently, at Micro-Bit Division of Control Data Corporation, he worked on various aspects of electron-beam accessed computer memories based on oxide charge storage in large area MOS devices, including high-dose electron beam effects on MOS devices, Si-SiO₂ interface state measurements, and packing density issues. At Atlantic Richfield, he helped develop a new R&D laboratory, and was in charge of electron probe microanalysis.

Joseph K. Reynolds received his Bachelor of Science Degree with Honors in Physics from The California Institute of Technology. During the summers of '87 and '88, he worked at Motorola's Advanced Product Research and Development Lab as an assistant process engineer. Kurth then spent two summers before graduation as an academic part time employee in Bill Kaiser's research group at JPL. He played a large role in the development of bulk micromachining and tunnel sensor capabilities at JPL during this time. This effort included the design and fabrication of an electron tunneling accelerometer and Golay Cell infrared detector. After graduation, Kurth continued work at JPL's

Microdevices laboratory and has collaborated on a neural probe development program, and on an improved Golay Cell. He has focused on a second generation tunneling accelerometer with high sensitivity (nano-g) and high bandwidth (5 kHz). A prototype device has been fabricated and is now being tested for application for undersea acoustics. When the accelerometer program is concluded, Kurth intends to move to a graduate research program, while continuing to work on novel sensor development. Kurth has co-authored 2 patent applications and 7 technical publications.

Judith A. Podosek has ten years of processing experience. She began her technical experience at The Aerospace Corporation where she fabricated and characterized semiconductor lasers. She also operated and maintained a Liquid Phase Epitaxy furnace used in the growth of GaAs/AlGaAs laser materials. In 1987 she joined the Photonics group at JPL as a processing engineer. She continued to work with semiconductor laser materials, both processing and using a Metal Organic Chemical Vapor deposition system to grow GaAs/AlGaAs laser materials. In 1990 she joined Bill Kaiser's research group and began working on tunneling sensors with Tom Kenny. Her primary responsibility has been assisting in the development of the tunneling infrared sensor, for which she was co-recipient of the 1993 R+D 100 Award. Judi is the co-author of a patent application and five technical publications.

Erika C. Vote received her Bachelor of Science Degree in Electrical Engineering from the Colorado School of Mines in 1992. Between college years, she spent her summers at JPL as an engineering intern, performing various tasks, including the fabrication of tunneling sensors for application as infrared sensors. After receiving her degree in 1992, she became a member of Tom Kenny's research group, where she continued the fabrication of new designs of the tunneling infrared sensor, and for which she was co-recipient of the 1993 R+D 100 Award. She also participates in work on tunneling magnetometers and deformable optical elements. Erika is co-author of one patent application and four technical publications.

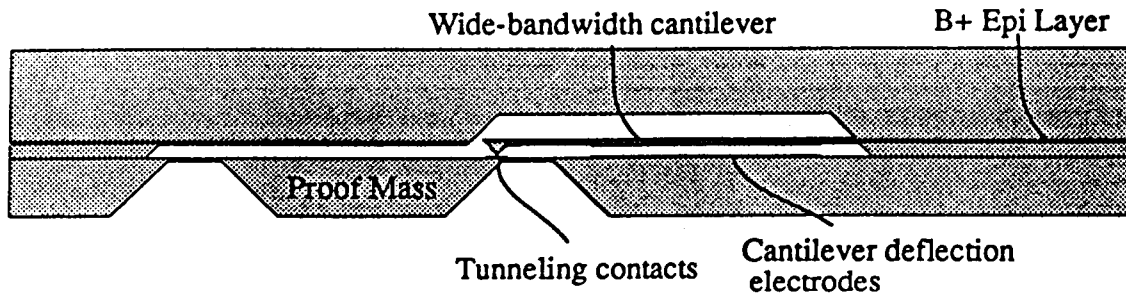


Fig. 1 This drawing shows the design concept for the tunneling accelerometer. A wide-bandwidth cantilever is controlled by the feedback circuit to follow the motion of the proof mass. Since the resonant frequency of the cantilever greatly exceeds that of the proof mass, feedback output signals at frequencies above and below the resonant frequency of the proof mass may be obtained. In this design the electrode gaps are about $15\ \mu\text{m}$, and the tip is about $15\ \mu\text{m}$ in height. The mass is $7\ \text{mm} \times 7\ \text{mm} \times 200\ \mu\text{m}$ and has a resonant frequency of $100\ \text{Hz}$.

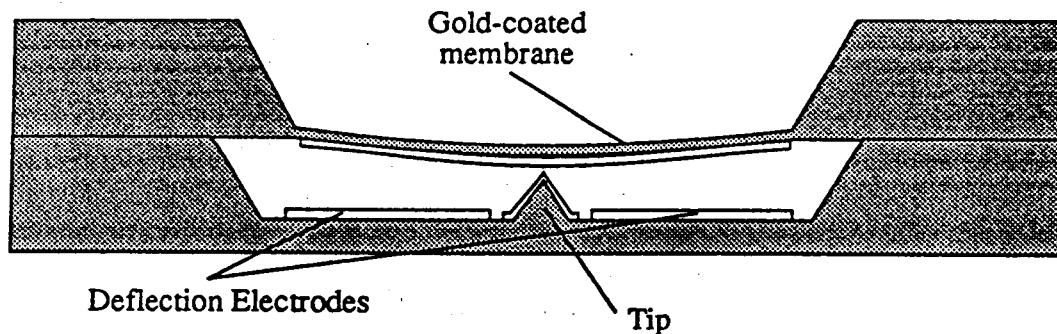


Fig. 2 This drawing shows the design of the membrane transducer. A gold-coated silicon nitride membrane is electrostatically deflected to within tunneling range of a micromachined tip. Variations in external forces applied to the membrane are canceled by feedback-generated variations in deflection force so as to keep the membrane in the same place. In this design, the gap between deflection electrode and membrane is about $50\ \mu\text{m}$, and the tip is about $50\ \mu\text{m}$ tall. The membrane is $2\ \text{mm} \times 2\ \text{mm} \times 0.5\ \mu\text{m}$.

Fig. 3 This SEM micrograph shows a typical micromachined silicon tip which results from the fabrication process. The lithographically-patterned gold electrodes for tunneling to the tip and for deflection of the transducer element are shown as well.

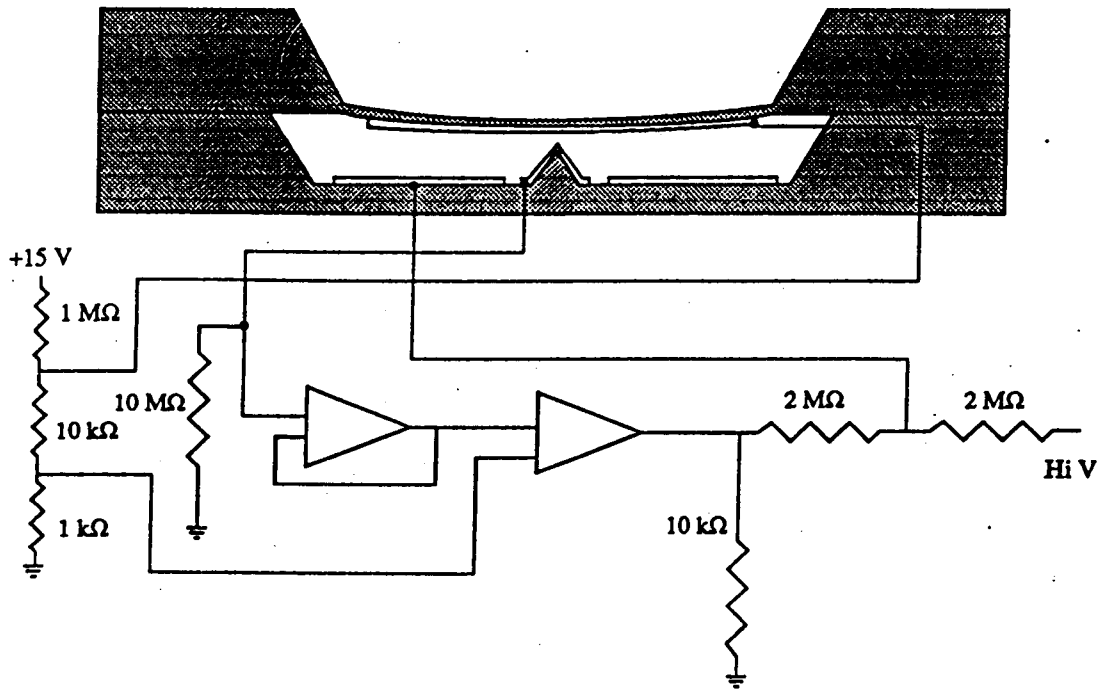


Fig. 4 This drawing shows the feedback circuit that is used to control the tunneling transducer. A bias of 163 mV is applied to a 10 MΩ resistor in series with the tunneling tip. The appearance of a tunneling current results in a voltage drop at the input of the preamplifier, which is operated in follower configuration. A second amplifier compares the measured voltage with a reference value and produces an error signal. The error signal is added to a high-voltage offset and applied to the deflection electrode.

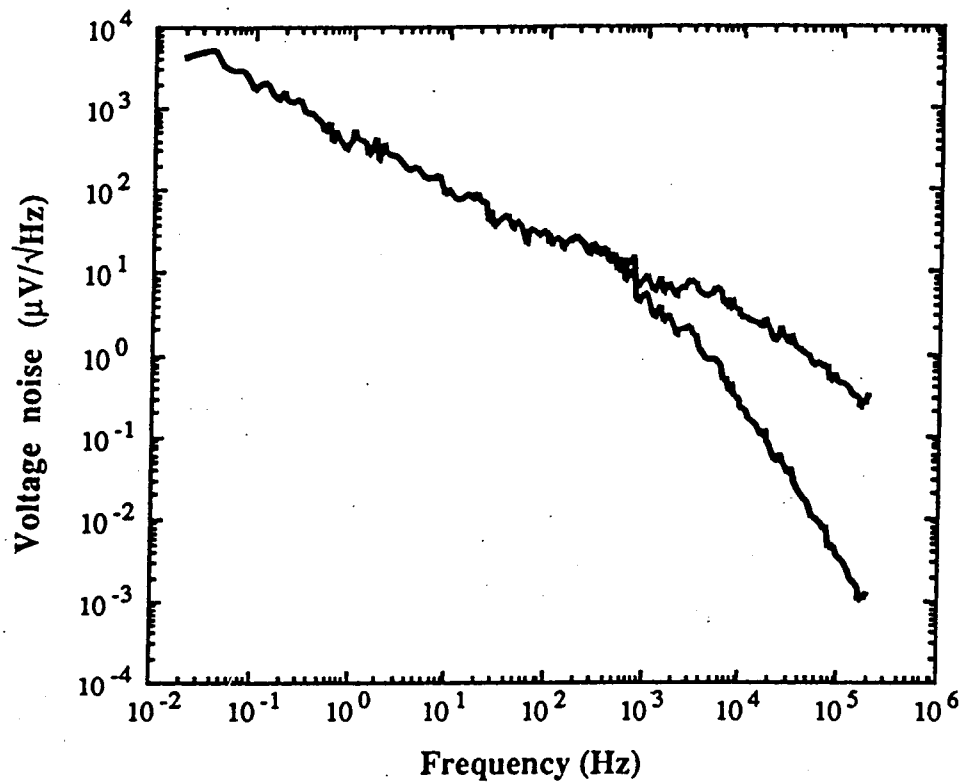


Fig. 5 This plot shows the measured voltage noise at the output of the feedback loop during operation of a tunneling transducer. The upper curve is recorded at the output of the error amplifier, while the lower curve is recorded at the deflection electrode. The noise at the deflection electrode is reduced by feedback loop resistance and stray capacitance combining to produce a low-pass filter at approximately 1 kHz.

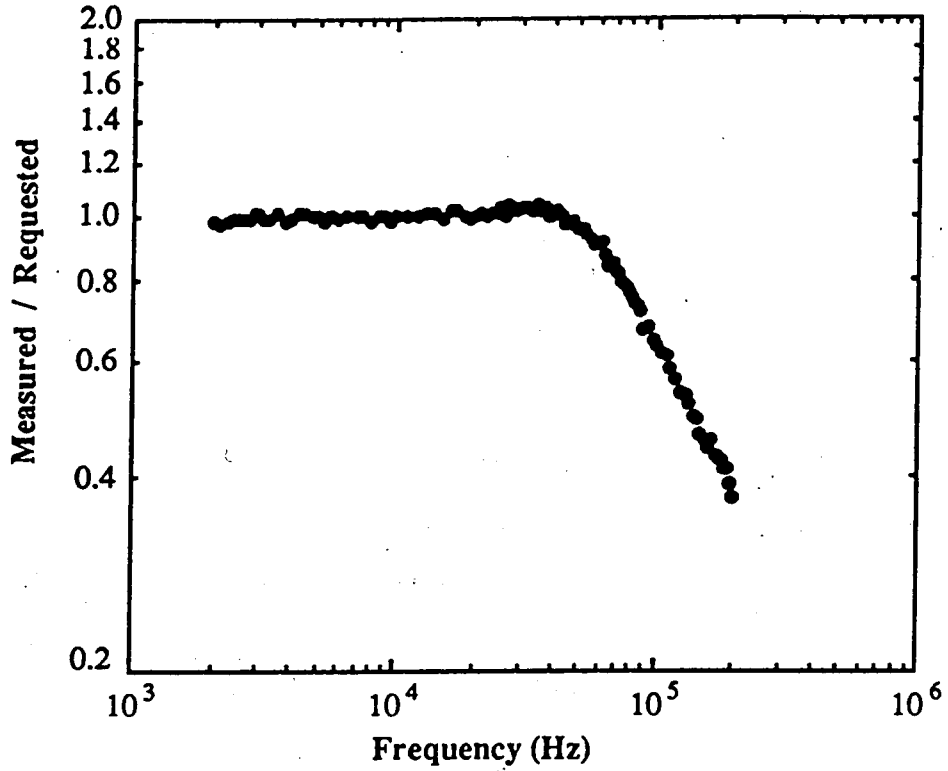


Fig. 6 This plot shows the ratio of measured modulation to input white noise modulation in the tunneling current as a function of frequency for frequencies between 2 kHz and 200 kHz. The feedback control system is able to reproduce the input white noise modulation at all frequencies up to 50 kHz.

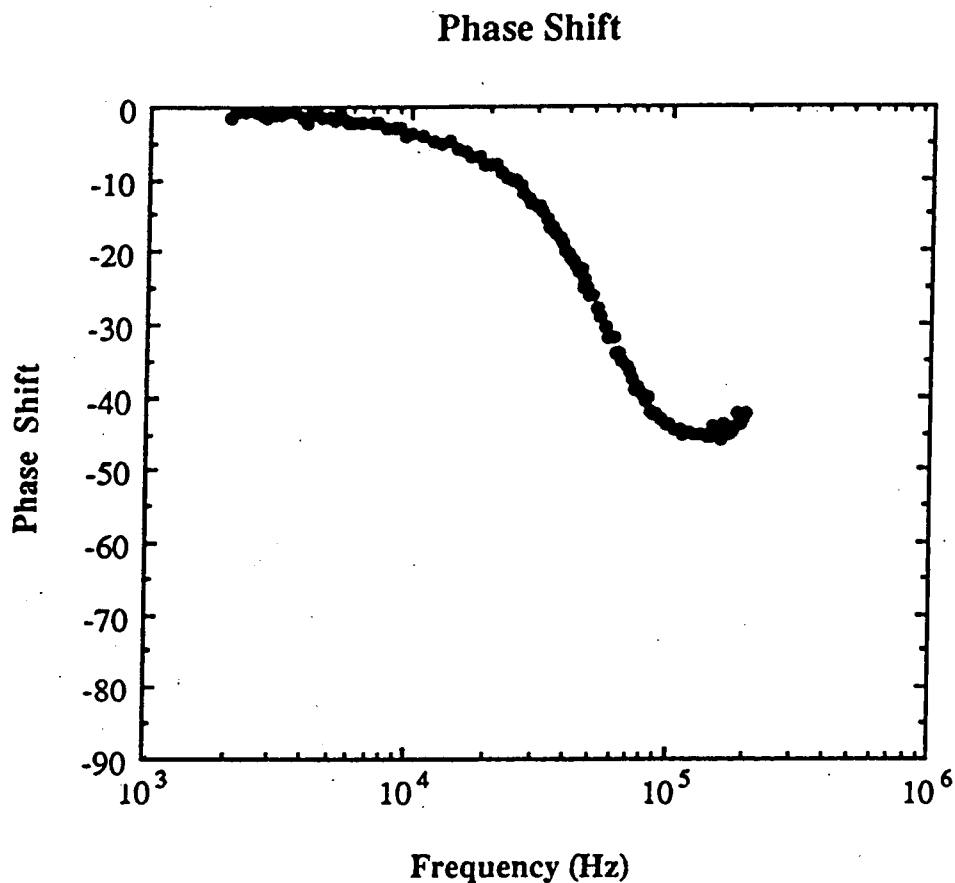


Fig. 7 This plot shows the phase shift between the measured and requested oscillation in tunneling current for frequencies between 2 kHz and 200 kHz. The phase shift is less than 5 degrees for frequencies below 10 kHz, but increases to 30 degrees at 50 kHz. Coupling between the noise generator and the transducer leads to errors in this measurement above 100 kHz.